Radiological Physics and Technology
https://doi.org/10.1007/s12194-020-00577-0

Comparison of dosimetric parameters of small-field electron beams between Advanced Markus, Semiflex 3D, and Diode E responses

Mohammad Reza Bayatiani[1] · Akbar Aliasgharzadeh[2] · Fatemeh Seif[1] · Fatholah Mohaghegh[1] · Fatemeh Fallahi[2]

Received: 18 March 2019 / Revised: 11 May 2020 / Accepted: 21 May 2020

Abstract
The usage of dosimetry of small fields in radiotherapy to measure radiation dose is difficult because of high-dose gradients, lateral electronic disequilibrium, and detector volume effects. In this study, three dosimeters namely, Markus, Semiflex 3D, and Diode E were tested using the Elekta-accelerator electron beams. The electron beam parameters, penumbra, and output factor were determined using these dosimeters for each field size and energy. According to the results, Diode E and Advanced Markus exhibited the greatest difference in Rq among the electron beam parameters. Furthermore, the greatest difference in penumbra was observed between Diode E and Advanced Markus for the field size of 3 cm^2 at 10 MeV. In terms of output factor, three dosimeters exhibited the greatest difference between Diode E and Advanced Markus for the field size of 3 cm^2 at 10 MeV. The findings indicate that the Semiflex 3D can be regarded as an appropriate dosimeter for electron small-field dosimetry.

Keywords Dosimetry · Electron beam · Energy · Output factor · Penumbra · Small field

1 Introduction

Electron beam therapy is a modality for delivering precise radiation doses to superficial tumors. This therapeutic method is also important for the treatment of superficial lesions in various organs, as well as the eyes and lips. Electron beam parameters, including R_{100}, R_{50}, E_{P0}, E_0, and R_q, as well as the penumbra, are important for electron therapy and can be obtained via relative dosimetry measurements. The accuracy of the measurement of these parameters is dependent on the physical characteristics of the dosimetry chamber [1–3].

Perturbations in the environment can be caused by differences in atomic number, sensitive volume dimensions, density, and other physical properties of the dosimetry chamber. Such perturbations lead to uncertainties in small-field dosimetry results [4, 5]. These properties, as well as electron disequilibrium and high-gradient dosing, can modify the central-axis dose, thereby altering the electron beam parameters [6–8].

Based on experimental and Monte Carlo methods, previous studies have investigated various parameters such as detector type and volume that affect the dosimetry of photon beams in small fields [9–12]. However, little attention has been given to electron beams. Additionally, various types of specialized dosimetry equipment may not be available in some clinics. Therefore, it is essential to evaluate the abilities of different dosimeters under various conditions, such as small fields and various energy ranges for electron beams.

In this study, electron beam parameters were evaluated at three energy levels of 10, 15, and 18 MeV in small (i.e., 3×3 to 5×5 cm^2 with an applicator size of 6×6 cm^2) and large (i.e., 6×6, 10×10, 14×14 and 20×20 cm^2) fields using three dosimeters: Semiflex 3D, Diode E, and the plane-parallel ionization chamber of Advanced Markus (as a reference dosimeter).

Semiflex 3D was released in 2015 and has recently entered the dosimetry field. However, its responses in small electron fields have not been thoroughly studied and compared to the responses of other dosimeters. In this study, we examined the Semiflex 3D chamfer response by comparing it

✉ Fatemeh Fallahi
fallahi.1984@yahoo.com

[1] Department of Medical Physics and Radiotherapy, Arak University of Medical Sciences and Khansari Hospital, Arāk, Iran

[2] Department of Medical Physics, School of Paramedical Sciences, Kashan University of Medical Sciences, Kashan, Iran

Published online: 20 July 2020

to the responses of two other detectors to assess the accuracy of its response in small electron fields.

2 Materials and methods

2.1 Dosimeters

In this study, three dosimeters, namely Advanced Markus (model: 34045), Semiflex 3D (model: 31021), and Diode E (model: 60017), manufactured by the German PTW company were used for dosimetry testing. The characteristics of these dosimeters are listed in Table 1.

A voltage of + 400 V was applied to the Semiflex 3D chamber, which was positioned axially in a dosimetry phantom. Additionally, a voltage of + 300 V was applied to the plane-parallel ionization chamber of Advanced Markus.

2.2 Linear accelerator and phantom

In this study, we utilized the Elekta Precise linear accelerator with operating energy levels of 10, 15, and 18 MeV. Measurements were performed in an MP3-M tank (water phantom) with a size of $50 \times 50 \times 40.8$ cm^3 that was manufactured by PTW.

2.3 Measurements

In the large fields, measurements were performed using applicator sizes of 20×20, 14×14, 10×10, and 6×6 cm^2. Small fields with sizes of 3×3, 3.5×3.5, 4×4, 4.5×4.5, and 5×5 cm^2 were produced using square Cerrobend cutouts inserted into the end of a 6×6 cm^2 applicator. The source surface distance was set to 100 cm. Data obtained through a PTW TBA control unit and PTW Unidose electrometer were transferred to the MEPHYSTO mc^2 software for analysis. Subsequently, percentage depth dose (PDD) curves were drawn according to the TRS 398 protocol and electron beam parameters, such as R_{100}, R_{50}, R_q, E_0, and E_{P0}, were extracted for all investigated field sizes and energy levels.

Transverse dose profiles were obtained by determining the maximum depth of dose (d_{max}) for each energy level and field size, then placing the dosimeters in the phantom at a depth equal to d_{max}. Penumbras were then extracted from these profiles. Widths in the range of 20–80% were considered for the penumbras. Output factors were determined by the Advanced Markus, Diode E, and Semiflex 3D dosimeters. The output factors for all field sizes at energy levels of 10, 15, and 18 MeV were obtained by the following equation:

$$\text{Output factor} = \frac{D_{\text{field}}}{D_{\text{ref}}},$$

where D_{field} is the dose at d_{max} in the desired field and D_{ref} is the dose at d_{max} in the reference field (10×10 cm^2).

Plane-parallel ionization chambers are recommended for the calibration and dosimetry of electron beams in clinics [13–15]. Accordingly, in this study, for all measurements, the plane-parallel ionization chamber of Advanced Markus was selected as the reference dosimeter. The results obtained from this dosimeter were compared with those obtained from Semiflex 3D and Diode E. It is noteworthy that this is the first attempt to compare the Semiflex 3D dosimeter to other dosimeters.

Table 1 Characteristics of Advanced Markus, Semiflex 3D, and Diode E PTW dosimeters

Detectors/specifications	Advanced Markus	Semiflex 3D	Diode E
Type of product	Vented plane-parallel ionization chamber	Vented cylindrical ionization chamber	p-type silicon diode
Sensitive volume	0.02 cm^3 Radius 2.5 mm Depth 1 mm	0.07 cm^3 Radius 2.4 mm Length 4.8 mm	0.03 mm^3 1 mm^2 circular (≅0.56 mm) 30 µm thick Diameter 7 mm Length 45.5 mm
Total wall/window area density	106 mg/cm^2, 1.3 mm (protection cap included)	84 mg/cm^2	140 mg/cm^2
Entrance window/foil Wall of sensitive volume	0.03 mm PE (polyethylene CH2), 2.76 mg/cm^2	0.57 mm PMMA, 1.19 g/cm^3 0.09 mm graphite, 1.85 g/cm^3	0.3 mm RW3, 1.045 g/cm^3 0.4 mm epoxy
Direction of incidence	Perpendicular to chamber plan	axial, radial	axial
Radiation quality	2–45 MeV electrons	9–45 MeV electrons	6–45 MeV electrons
Field size	3×3 cm^2 to 40×40 cm^2	2.5×2.5 cm^2 to 40×40 cm^2	1×1 cm^2 to 40×40 cm^2

3 Results

3.1 Electron PDD parameters

Electron beam parameters, namely R_{100} (the depth at which the dose is 100% of the maximum dose), R_{50} (the depth at which the dose is 50% of the maximum dose), R_q (the depth at which the tangent through the dose inflection point intersects the maximum dose level), E_0 (the mean energy at the phantom surface), and E_{P0} (the most probable energy level at the phantom surface), are listed in Tables 2, 3 and 4 for all field sizes and energies for Advanced Markus (AM), Semiflex 3D (SF3D), and Diode E (Si-D).

One can see that the electron beam parameters decrease with decreasing field dimensions. Additionally, R_{100}, R_{50}, and R_q are shifted toward the phantom surface. Furthermore, these parameters increase with increasing energy and penetrate deeper into the phantom.

A comparison of the electron beam results obtained from Advanced Markus to those obtained from Semiflex 3D and Diode E revealed that the greatest difference was in the parameter R_q (2 mm) between Diode E and Advanced Markus with a field size of 3×3 cm^2 at an energy level of 18 MeV.

3.2 Penumbra

The penumbras obtained from the three dosimeters for all fields at beam energies of 10, 15, and 18 MeV are listed in Table 5.

According to Table 5, penumbra increases with increasing energy and field size. However, these changes are more significant for increases in energy. Regarding Advanced Markus, penumbra increased from 11.5 mm to 13.8 mm, 11.8 mm to 15.1 mm, and 12.0 mm to 16.6 mm for field sizes ranging from 3×3 to 20×20 cm^2 at the three beam energies of 10, 15, and 18 MeV, respectively. However, these changes were more apparent with increases in energy.

A comparison of Advanced Markus to Semiflex 3D and Diode E in terms of penumbra values revealed that the greatest difference (1.1 mm) occurred between Diode E and Advanced Markus with a field size of 3×3 cm^2 at an energy level of 10 MeV (Fig. 1).

3.3 Output factor

The output factors obtained for Advanced Markus, Semiflex 3D, and Diode E are listed in Fig. 2.

As shown in Fig. 2, the output factors increase with increasing energy and field size.

A comparison of the output factors (Fig. 3) between the three dosimeters in the evaluated fields and beam energy levels revealed that the greatest difference (2.1%) occurred between Advanced Markus and Diode E with a field size of 3×3 cm^2 at an energy level of 10 MeV.

Table 2 Results for R_{100}, R_{50}, R_q, E_0, and E_{P0} obtained from SF3D, AM and Si-D dosimeters in the evaluated fields at 10 MeV

Energy 10 MeV	3×3[a]	3.5×3.5[a]	4×4[a]	4.5×4.5[a]	5×5[a]	6×6[b]	10×10[b]	14×14[b]	20×20[b]
AM									
R_{100} (mm)	15.5	17	18.1	19	20	20.99	21.5	23	23.9
R_{50} (mm)	37.52	38.6	38.65	39	39.23	39.23	41	41.6	41.77
R_q (mm)	25.28	27.21	27.95	28.41	28.54	28.81	30.4	30.44	30.44
E_0 (MeV)	8.74	9	9.01	9.09	9.14	9.15	9.53	9.7	9.73
E_{p0} (MeV)	9.8	9.83	9.83	9.85	9.9	9.91	10.14	10.42	10.42
SF3D									
R_{100} (mm)	15.7	18	18	19.1	20.8	21	21	21.8	23
R_{50} (mm)	38	38.2	38.24	39.3	39.4	39.53	41	41.1	41.12
R_q (mm)	27.1	28.3	28.32	28.99	29.19	29.69	29.7	29.71	29.72
E_0 (MeV)	8.86	9.14	9.14	9.16	9.19	9.21	9.5	9.56	9.58
E_{p0} (MeV)	9.87	9.9	9.92	10.04	10.06	10.07	10.68	10.7	10.7
Si-D									
R_{100} (mm)	16.2	18.23	18.4	20	21	21.11	22	23.01	23.5
R_{50} (mm)	38.61	38.7	38.72	39.5	39.8	39	40.94	41.2	41.5
R_q (mm)	26.2	27.4	28.59	28.64	28.71	28.83	30.45	30.5	30.51
E_0 (MeV)	9	9.11	9.13	9.2	9.3	9.32	9.54	9.54	9.59
E_{p0} (MeV)	9.94	9.87	9.94	9.97	9.98	9.98	10.4	10.42	10.42

[a]Open field, with the cutout

[b]Open field, with the applicator

Table 3 Results for R_{100}, R_{50}, R_q, E_0, and E_{P0} obtained from SF3D, AM and Si-D dosimeters in the evaluated fields at 15 MeV

Energy 15 MeV	3×3[a]	3.5×3.5[a]	4×4[a]	4.5×4.5[a]	5×5[a]	6×6[b]	10×10[b]	14×14[b]	20×20[b]
AM									
R_{100} (mm)	16	17.2	20	21	22	23	24.1	24.2	24.3
R_{50} (mm)	52.2	55.2	56.65	57.85	58.8	59.6	61.1	61.2	61.32
R_q (mm)	30.15	34.02	36.36	38.47	40.34	41.91	43.21	43.52	43.6
E_0 (MeV)	12.2	12.86	13.2	13.48	13.69	13.88	14.24	14.29	14.29
E_{p0} (MeV)	14.5	14.79	14.89	14.97	14.99	15	15.13	15.17	15.17
SF3D									
R_{100} (mm)	16.1	18.4	19.5	21.2	22.2	23.5	24.2	24.3	24.37
R_{50} (mm)	52.71	54.8	55.4	57.41	57.78	58.67	60.4	60.64	60.8
R_q (mm)	30.75	34.63	36.07	38.83	40.96	41.24	41.68	41.72	41.75
E_0 (MeV)	12.28	12.77	12.91	13.38	13.46	13.67	14.08	14.13	14.16
E_{p0} (MeV)	14.87	14.88	14.89	14.9	15	15.4	15.75	15.79	15.79
Si-D									
R_{100} (mm)	16.3	18.5	20.5	21.4	22	23	25.1	25.2	26
R_{50} (mm)	52.81	55.17	55.95	57.5	58.04	58.12	60.85	61.02	61.14
R_q (mm)	32.13	34.57	36.48	39.96	40.10	43.32	41.52	41.61	41.64
E_0 (MeV)	12.3	12.85	13.04	13.38	13.52	13.54	14.18	14.22	14.25
E_{p0} (MeV)	14.54	14.96	14.99	15	15.11	15.2	15.87	15.91	15.91

[a]Open field, with the cutout

[b]Open field, with the applicator

Table 4 Results for R_{100}, R_{50}, R_q, E_0, and E_{P0} obtained from SF3D, AM and Si-D dosimeters in the evaluated fields at 18 MeV

Energy 18 MeV	3×3[a]	3.5×3.5[a]	4×4[a]	4.5×4.5[a]	5×5[a]	6×6[b]	10×10[b]	14×14[b]	20×20[b]
AM									
R_{100} (mm)	19	21	21.3	21.5	22.8	25.1	26.2	26.3	27
R_{50} (mm)	57.45	60	62.6	63.8	64.6	68	69.3	69.6	70
R_q (mm)	31.55	36.3	38.41	39.82	41.7	46.83	49.3	49.49	49.49
E_0 (MeV)	13.38	14	14.59	14.88	15.04	15.86	15.9	15.99	16.01
E_{p0} (MeV)	16.22	16.38	16.68	16.93	16.96	17.27	17.39	17.46	17.46
SF3D									
R_{100} (mm)	19	21.3	21.5	22	23	25.3	26	26.1	27
R_{50} (mm)	58	60.24	63.4	65	66.3	67.5	68.8	69.1	69.3
R_q (mm)	31.9	36.6	39.44	39.67	43.5	47.3	50.9	50.97	50.69
E_0 (MeV)	13.51	14.43	14.77	15.15	15.44	15.75	16	16.1	16.12
E_{p0} (MeV)	16.36	16.42	16.77	17.31	17.32	17.33	17.36	17.37	17.38
Si-D									
R_{100} (mm)	19.1	21.23	21.7	21.8	23.01	25.8	27.2	27.3	28.87
R_{50} (mm)	59.2	60.1	63.2	64.4	65.2	67.4	68.9	69	69.2
R_q (mm)	33.55	37.37	39.61	39.83	42.6	47.42	51	51.21	51.22
E_0 (MeV)	13.8	14.6	14.71	14.99	15.18	15.78	16	16.1	16.1
E_{p0} (MeV)	16.68	17	17.08	17.23	17.26	17.3	17.33	17.35	17.35

[a]Open field, with the cutout

[b]Open field, with the applicator

Table 5 Penumbras obtained by SF3D, AM and Si-D dosimeters in all assessed fields at 10, 15, and 18 MeV

Field (cm^2)	80–20% penumbra (mm)								
	10 MeV			15 MeV			18 MeV		
	AM	SF3D	Si-D	AM	SF3D	Si-D	AM	SF3D	Si-D
3×3[a]	11.5	10.6	10.4	11.8	11.1	10.9	12.0	11.1	11.8
3.5×3.5[a]	11.2	11.2	11.0	12.7	12.1	11.8	12.9	12.1	12.9
4×4[a]	11.4	11.8	11.0	12.8	12.8	12.1	13.5	13.8	13.2
4.5×4.5[a]	12.3	11.9	11.9	13.8	13.3	12.8	14.1	13.8	14.1
5×5[a]	12.4	12.6	12.2	14.2	14.1	13.2	14.8	14.5	14.4
6×6[b]	13.1	13.0	12.6	14.5	14.1	13.6	14.9	14.8	14.8
10×10[b]	13.3	13.1	12.9	14.3	14.4	13.6	16.1	15.5	15.3
14×14[b]	13.7	13.1	13.0	14.7	14.7	13.8	16.5	15.9	15.6
20×20[b]	13.8	13.1	13.1	15.1	14.9	14.6	16.6	15.9	16.1

[a]Open field, with the cutout

[b]Open field, with the applicator

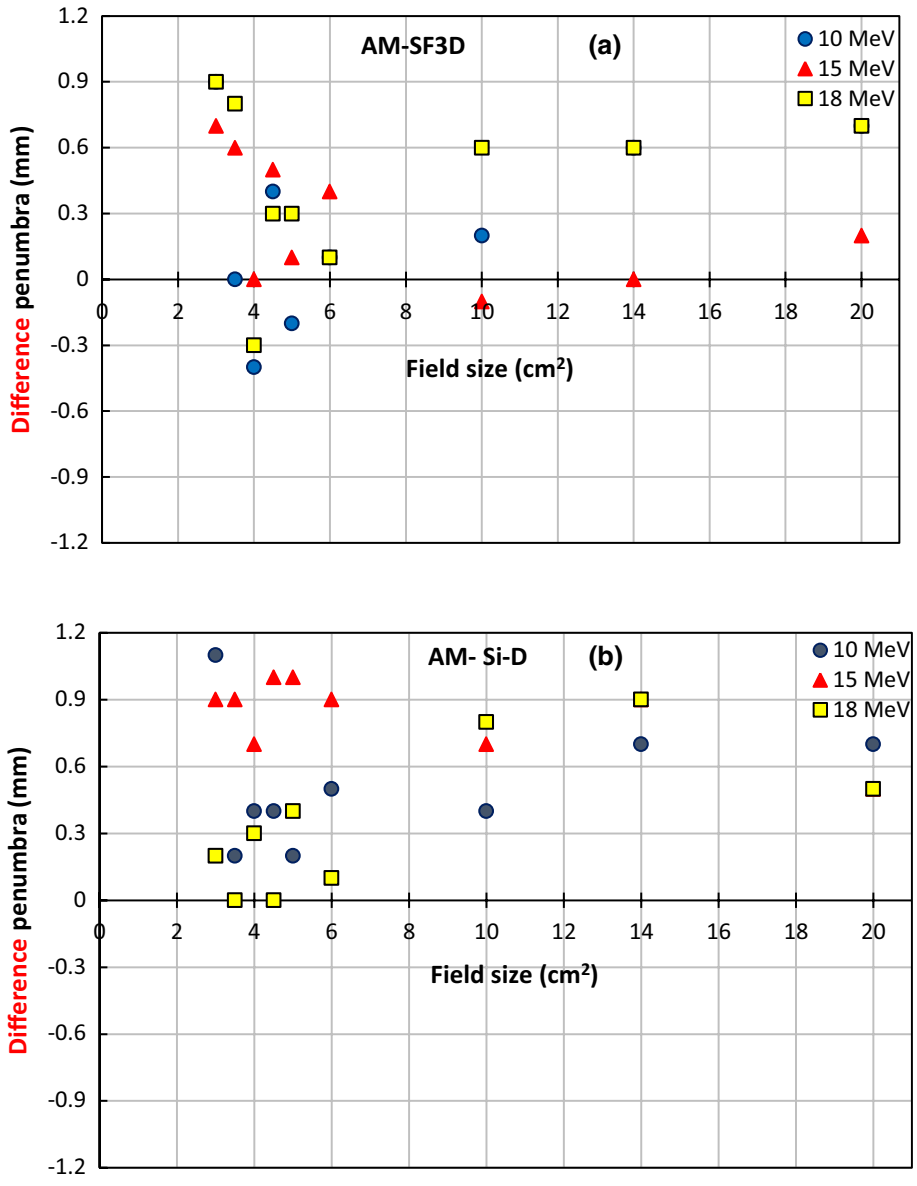

Fig. 1 **a** Penumbra differences between the SF3D and AM dosimeters, and **b** between the Si-D and AM dosimeters in all assessed fields at 10, 15, and 18 MeV

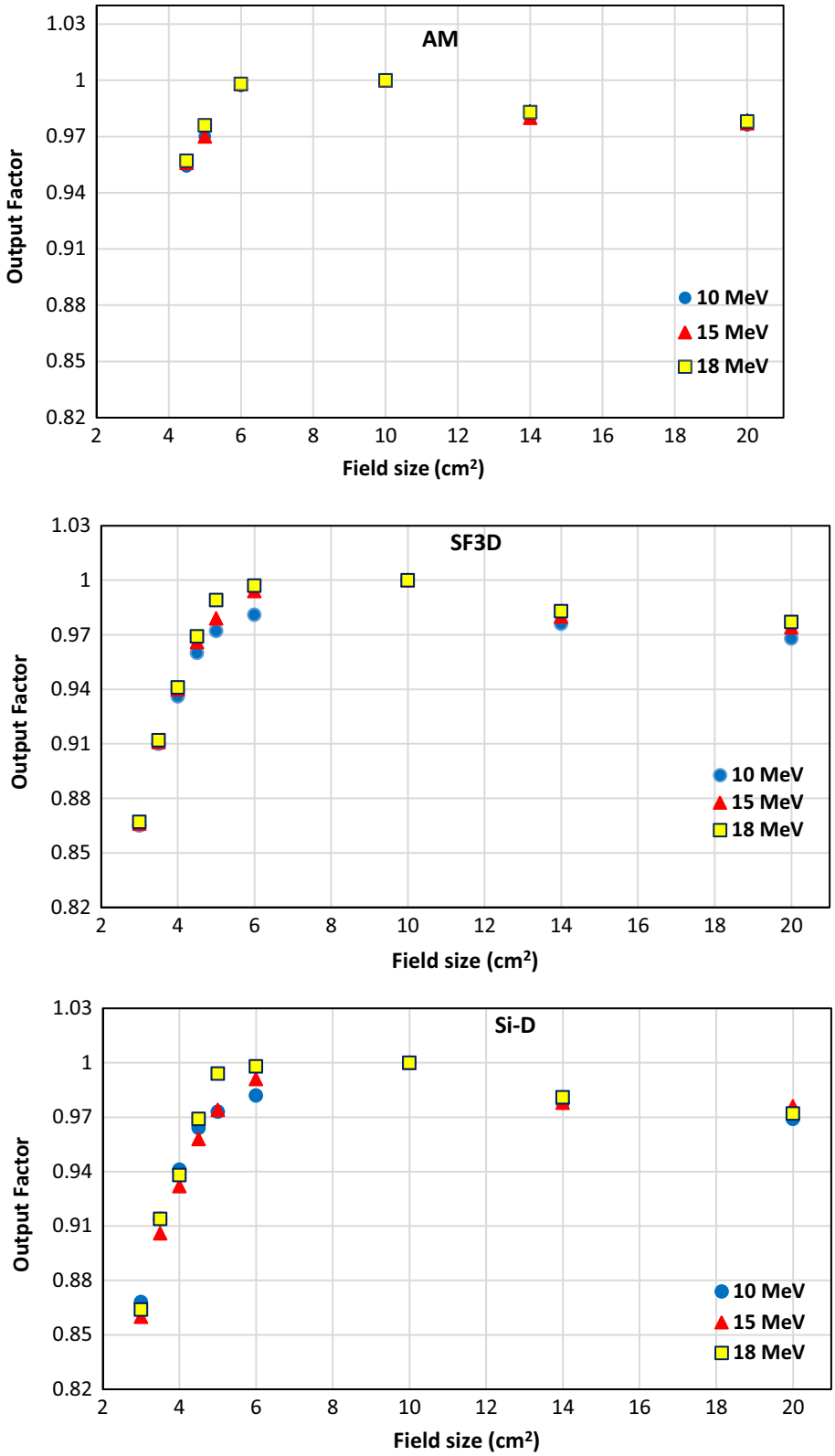

Fig. 2 Output factors obtained from SF3D, AM and Si-D in the evaluated fields at 10, 15, and 18 MeV

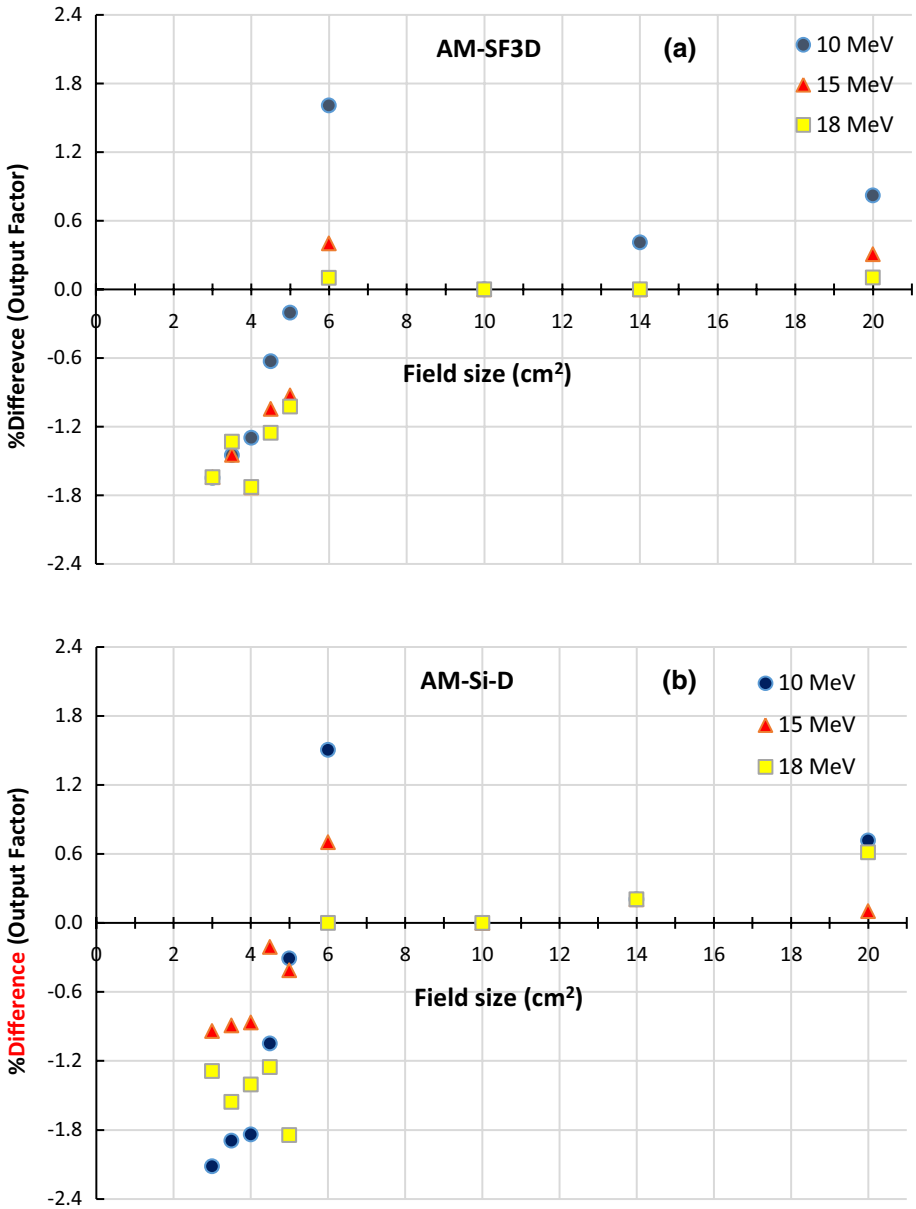

Fig. 3 **a** Output factor differences between the SF3D and AM dosimeters, and **b** between the Si-D and AM dosimeters in all assessed fields at 10, 15, and 18 MeV

4 Discussion

4.1 Electron PDD parameters

After comparing the results for the various evaluated fields and energy levels, it was determined that electron PDD parameters are dependent on field size and energy level because they tend to increase with increasing energy and penetrate deeper into the phantom. A reduction in field size leads to a reduction in the R_{100}, R_{50}, and R_q parameters and shifts them toward the surface of the phantom. With a field size change from 3×3 to 20×20 cm^2 at an energy level of 10 MeV, the values of R_{100}, R_{50}, and R_q for the chamber of Advanced Markus decreased from 23.9 mm to 15.5 mm, 41.77 mm to 37.52 mm, and 30.44 mm to 25.28 mm, respectively. Furthermore, a decrease in the size of the field also led to decreasing values of E_0 and E_{P0}.

These changes in small fields may be caused by lateral electronic disequilibrium because the decreased field size results in a reduction of lateral scattered electrons. Accordingly, the electrons lose their energy at a shallower depth in the phantom. Moreover, certain parameters, such as R_{100}, R_{50}, and R_q, approach the surface. Amin et al. evaluated the challenges related to the dosimetry of small-field electron beams and reported that a reduction in field size resulted in a shift of the position of d_{max} toward the surface of the phantom [6].

Furthermore, Xu et al. evaluated the dosimetry of small fields and concluded that a reduction in cutout diameter also reduces d_{max} and R_q [16]. Khaledi et al. demonstrated that

the use of smaller cutouts resulted in reductions in the depths of R_{100}, R_{90}, R_{80}, and R_{50}. This reduction was the most significant for R_{100} and R_{90} [17].

In a study by Arunkumar et al., decreasing field size led to shifts of R_{100} and R_{50} toward the surface of the phantom, which were more significant at higher energy levels [18]. In this regard, the results of the studies mentioned above are in congruence with our findings.

In previous studies, Advanced Markus chamber responses have been compared to the results of Monte Carlo simulation and film dosimetry in electron fields. It was found that Advanced Markus provides results comparable to these other methods [7, 19, 20]. In this study, the Advanced Markus chamber was selected as a reference chamber, and the responses of two other detectors were compared to those of the Advanced Markus chamber.

As shown in the results above, the greatest difference was observed in terms of R_q (2 mm) between Diode E and Advanced Markus. Discrepancies in the responses of the three dosimeters may be caused by differences in the sensitive volume, material, and type of the dosimeters (Table 1). In general, there were few differences between the dosimeters at various field sizes, which is indicative of similar performance between the three dosimeters.

4.2 Penumbra

The results of this study are in agreement with those obtained by Sampaio et al. and Polston et al., who reported that penumbra increases with an increasing field size [21, 22]. According to Fig. 1, for the majority of field sizes, the differences between the responses of Diode E and Advanced Markus were greater than those between Semiflex 3D and Advanced Markus, but the responses of the chambers were very similar overall.

The differences may be caused by the different structures of Diode E and Advanced Markus. The former is a semiconductor detector, whereas the latter is a plane-parallel ionization chamber. Given that the greatest difference between the responses of the dosimeters was related to the smallest evaluated field, this difference can be attributed to variation in the sensitive volumes of the dosimeters.

The sensitive volume radii of Advanced Markus and Semiflex 3D are 2.5 mm and 2.4 mm, respectively. Diode E has a much smaller sensitive volume radius of 0.56 mm, leading to the indication of less penumbra.

4.3 Output factor

The evaluation of output factors revealed that the output factors increased with increasing field size as well as with increasing energy levels. These changes can be explained by the scattering of electrons in water and collimators. In general, electrons have lower scattering in water and collimators with small fields and low energy levels. Our findings are in congruence with the results obtained by Sampaio et al., who concluded that output factors decrease with decreasing field size and energy levels [21]. However, Di Venanzio et al. reported that output factors largely depend on the size of the field because they decrease with decreasing field size at a constant energy level [23].

Furthermore, the density of Advanced Markus is greater than that of Semiflex 3D. It is believed that the enhancement of density leads to an increase in dose readings for a given sensitive volume. However, as shown in Table 1, the output factor of Semiflex 3D was greater in small fields compared to that of Advanced Markus. This distinction may be caused by differences in the sensitive volumes of the chambers.

The sensitive volumes of the Advanced Markus and Semiflex 3D chambers are 0.02 cm^3 and 0.07 cm^3, respectively. Therefore, when measuring the output of the ionization chamber, lateral scatter disequilibrium leads to a greater output with a larger sensitive volume. However, there was a small difference between the responses of the two dosimeters, which may be a result of the small difference between the sensitive volumes of the two chambers. Based on these findings, we wish to measure the output factors of electron beams using two chambers with a greater difference in sensitive volume and evaluate the resulting variations.

For nearly all fields and energy levels, the output factor of Diode E was greater than that of the other two chambers. This may be a result of the over-response effect of the diode. As mentioned previously, Diode E is a semiconductor detector, whereas Advanced Markus and Semiflex 3D are ionization chambers with a different structure.

It should be noted that in electron fields, various factors, such as sensitive volume and high-density materials, have no considerable effects on the responses of dosimeters because these factors largely compensate for the impacts of each other.

Based on our comparisons of the three dosimeters in terms of output factor, the greatest difference (2.1%) was observed between Advanced Markus and Diode E for a field size of 3×3 cm^2 at an energy level of 10 MeV. This small difference can be attributed to lateral scatter disequilibrium and the difference in the sensitive volumes of the dosimeters. Overall, the differences were greater in the small fields compared to those in large fields.

Small differences in the range of 2% can be neglected in clinical practice [24]. Overall, the differences observed in our experiments were very small, and it can be concluded that the responses of the three dosimeters are very similar.

The Semiflex 3D dosimeter manufactured by PTW has recently been adopted for practical applications. However, it is necessary to evaluate the accuracy of its responses in small electron fields. In this study, the Semiflex 3D

dosimeter was examined with two other dosimeters, and its responses were compared to those of the Advanced Markus reference chamber, which was validated in previous studies by the Monte Carlo method and film dosimetry. The results of our comparisons demonstrated that the responses of Semiflex 3D are in agreement with those of the reference chamber. Therefore, Semiflex 3D can be used as a suitable dosimeter for the dosimetry of small electron fields (3×3 to 6×6 cm^2) at various energy levels (10, 15, and 18 MeV) in clinical practice. It should be noted that fields smaller than 3×3 cm^2 and energy levels higher than 18 MeV require further investigation. Additionally, individuals should always evaluate their equipment prior to clinical use to observe any significant differences and evaluate the clinical importance of results for their field based on specific techniques.

5 Conclusions

The selection of a suitable dosimeter for the measurement of electron parameters in small fields with lateral scatter disequilibrium is a critical issue. According to the cavity theory, the most prevalent cause of disruption in the dosimetry of small electron beams and photonic fields is electron disequilibrium. This problem is intensified by various parameters, such as sensitive volume radius, high-density material perturbation, and volume averaging effects.

These factors can increase or decrease dosimeter responses depending on the type of dosimeter. The results of this study indicate that these factors may compensate for the effects of one another. Therefore, they should not lead to any considerable differences in the responses of dosimeters in small electron fields. It was also determined that the response of 0.07 cm^3 of Semiflex 3D, which was released in 2015, shows no significant differences compared to the responses of other dosimeters in small fields. Therefore, this dosimeter should be suitable for small electron fields.

The Semiflex 3D dosimeter manufactured by PTW has recently been adopted for practical applications. In this study, the Semiflex 3D 0.07 cm^3 dosimeter was investigated in small electron fields (3×3 to 6×6 cm^2) at energy levels of 10, 15, and 18 MeV. It was found that its responses are in agreement with those of the Advanced Markus reference dosimeter. Therefore, the Semiflex 3D 0.07 cm^3 dosimeter is appropriate for the tested fields and energies.

Acknowledgements This manuscript is part of a research project No. 1395.45 of the Kashan University of Medical Sciences and research project No. 1232 of the Arak University of Medical Sciences, Iran.

Funding No funding was granted for this study.

Compliance with ethical standards

Conflict of interest All authors declare that they have no conflicts of interest.

Ethical approval This study did not involve any experiments with human participants or animals performed by any of the authors.

Informed consent Informed consent was obtained from all individuals participating in this study.

References

1. Butson M, et al. Reducing shield thickness and backscattered radiation using a multilayered shield for 6–10 MeV electron beams. Australas Phys Eng Sci Med. 2015;38(4):619–26.
2. Yeung W, Luk N, Yu K. Current tools of radiation therapy in treatment of skin cancer. Hong Kong J Dermatol Venereol. 2009;17(2):79–86.
3. Perez M, et al. Dosimetry of small electron fields shaped by lead. Australas Phys Eng Sci Med. 2003;26(3):119–24.
4. Pappas E, et al. Small SRS photon field profile dosimetry performed using a PinPoint air ion chamber, a diamond detector, a novel silicon-diode array (DOSI), and polymer gel dosimetry. Analysis and intercomparison. Med Phys. 2008;35(10):4640–8.
5. Scott AJ, et al. Characterizing the influence of detector density on dosimeter response in non-equilibrium small photon fields. Phys Med Biol. 2012;57(14):4461.
6. Amin MN, et al. Small field electron beam dosimetry using MOSFET detector. J Appl Clin Med Phys. 2010;12(1):50–7.
7. Khaledi N, et al. Monte Carlo investigation of the effect of small cutouts on beam profile parameters of 12 and 14 MeV electron beams. Radiat Meas. 2013;51:48–544.
8. Arunkumar T, et al. Impact of cutout off axis on electron beam dosimetric parameters. Technol Cancer Res Treat. 2012;11(2):141–7.
9. Huet C, et al. Characterization and optimization of EBT2 radiochromic films dosimetry system for precise measurements of output factors in small fields used in radiotherapy. Radiat Meas. 2012;47(1):40–9.
10. Stasi M, et al. The behavior of several microionization chambers in small intensity modulated radiotherapy fields. Med Phys. 2004;31(10):2792–5.
11. Papaconstadopoulos P, Tessier F, Seuntjens J. On the correction, perturbation and modification of small field detectors in relative dosimetry. Phys Med Biol. 2014;59(19):5937.
12. Benítez E, et al. Evaluation of a liquid ionization chamber for relative dosimetry in small and large fields of radiotherapy photon beams. Radiat Meas. 2013;58:79–86.
13. Di Venanzio C, et al. Characterization of a synthetic single crystal diamond Schottky diode for radiotherapy electron beam dosimetry. Med Phys. 2013;40(2):021712.
14. Lee SH, et al. Analysis of output factors with various detectors in small-field electron-beam radiotherapy. J Korean Phys Soc. 2012;60(5):875–80.
15. Song H, et al. Limitations of silicon diodes for clinical electron dosimetry. Radiat Prot Dosim. 2006;120(1–4):56–9.
16. Xu MM, Sethi A, Glasgow GP. Dosimetry of small circular fields for 6-MeV electron beams. Med Dosim. 2009;34(1):51–6.
17. Khaledy N, Arbabi A, Sardari D. The effects of cutouts on output, mean energy and percentage depth dose of 12 and 14 MeV electrons. J Med Phys. 2011;36(4):213.

18. Arunkumar T, et al. Electron beam characteristics at extended source-to-surface distances for irregular cut-outs. J Med Phys. 2010;35(4):207.
19. Aghdam MRH, et al. Monte Carlo study on effective source to surface distance for electron beams from a mobile dedicated IORT accelerator. J Radiother Pract. 2017;16(1):29–37.
20. Donmez Kesen N, et al. A comparison of TPS and different measurement techniques in small-field electron beams. Med Dosim. 2015;40(1):9–15.
21. Sampaio FG, et al. 8 and 10 MeV Electron beams small field-size dosimetric parameters through the Fricke xylenol gel dosimeter. IEEE Trans Nucl Sci. 2013;60(2):572–7.
22. Polston GK (2008) A dosimetric model for small-field electron radiation therapy. Ball State University
23. Di Venanzio C, et al. Radiotherapy electron beams collimated by small tubular applicators: characterization by silicon and diamond diodes. Phys Med Biol. 2013;58(22):8121.
24. Cygler J, et al. Practical approach to electron beam dosimetry at extended SSD. Phys Med Biol. 1997;42(8):1505.